Hindawi
International Journal of Antennas and Propagation
Volume 2022, Article ID 2653410, 8 pages
https://doi.org/10.1155/2022/2653410

Research Article

A 3D Printed Ka-Band High-Efficiency Wide-Slit Antenna Array for High-Power Microwave Applications

Liang Liu, Yu Yang, Shifeng Li, Xianghe Fang, Fanbao Meng, and Chuan Yu

Science and Technology on High Power Microwave Laboratory, Institute of Applied Electronics, CAEP, Mianyang 621900, China

Correspondence should be addressed to Chuan Yu; yuchuan@263.net

Received 15 January 2022; Revised 1 April 2022; Accepted 7 April 2022; Published 23 April 2022

Academic Editor: Renato Cicchetti

A Ka-band high-power waveguide wide-slit antenna array with high efficiency and high-power capacity is proposed in this paper. The antenna uses a waveguide vertical transition structure as a part of the feed network, which improves the compactness and power capacity of the antenna. A 2×8 antenna array was simulated, fabricated by 3D printed technology, and measured. The measured reflection coefficient is less than −10 dB in the range of 30.4–30.9 GHz, the tested gain at 30.8 GHz is 25.8 dB, and the corresponding aperture efficiency is larger than 80%. This antenna can be applied in high-power millimeter-wave systems.

1. Introduction

High-power microwave (HPM) is generally defined as electromagnetic waves with peak power higher than 100 MW in the frequency range of 1 to 300 GHz [1–3]. Recently, high-power technologies have been guided by the demand for microwave sources in communication systems, long-range radars, and new gas pedals to higher frequencies. According to published literature, Ka-band high-power microwave sources [4] have reached 500 MW. Horn antennas are often used in high-power microwave systems, but their low gain and large size are not conducive to practical scenarios. To improve the practicality and broaden the application range, the development of miniaturized and high-efficiency Ka-band high-power millimeter-wave antennas has become an urgent problem.

Traditional HPM antennas, such as Vlasov antennas [5], COBRA antennas [6–8], and large-aperture parabolic antennas [9], meet the needs of experiments and applications to some extent, but their large size, complex configuration, and low-radiation efficiency limit their applications. Later, radial spiral line array antennas [10], radial line slot arrays [11], and transmit-array antennas [12–16] were developed. These types of antennas have good performance but are particularly difficult to process when the wavelength of high-frequency electromagnetic waves becomes shorter. In addition, the feed network is complex and it is difficult to form a large array. Meanwhile, many Ka-band planar array antennas [17–19] have been reported in recent years, but no definitive study of their power capacity has been made.

Therefore, we propose a wide-slit antenna array consisting of a waveguide resonant cavity and a waveguide vertical transition structure. As a traditional transmission line structure, the rectangular waveguide has the advantages of easy processing, low transmission loss, and high-power capacity. It has been a commonly used large transmission structure in the field of high-power microwaves. Most traditional waveguide slot array antennas [20] use longitudinal offset slots with narrow slot widths. When it is applied to high-power microwaves, the electric field of the slot is too concentrated, which reduces the power capacity of the system. The slot feed is also chosen for the feed network, which further reduces the power capacity of the system. Therefore, this paper innovatively adopts the waveguide vertical conversion structure in the design process to avoid the slit structure, thus increasing the power capacity. The radiation structure takes the form of 2×2 radiating wide slits. The wide slit has a higher power capacity, and the closely arranged antenna surface has a more uniform current distribution, which can improve the aperture efficiency of

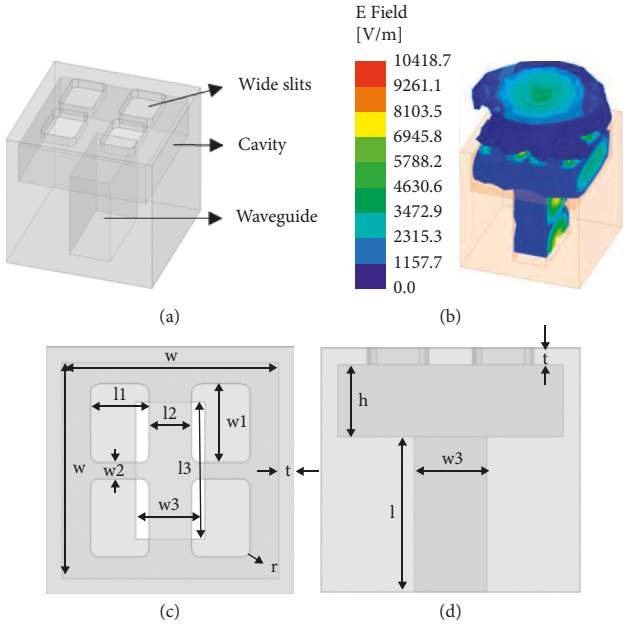

FIGURE 1: (a) Schematic, (b) electric field distribution, (c) top view, and (d) front view of the antenna unit. $w = 13.5$ mm, $h = 4.318$ mm, $l1 = 3.66$ mm, $w1 = 4.91$ mm, $l2 = 2.66$ mm, $w2 = 1.01$ mm, $l3 = 8.636$ mm, $w3 = 4.318$ mm, $t = 1$ mm, $r = 0.54$ mm, and $l = 9.28$ mm.

the antenna, reduce the size of the antenna, and facilitate the planarization and miniaturization design of the antenna. The antenna is fabricated by 3D printed technology. Recently, metal 3D printed technology [21–23] has been widely used in the fields of aerospace, automotive, medical applications, and manufacturing, as it shows great promise to complete almost any structural part of computer-aided drafting (CAD) and to increase processing speed while reducing production costs.

2. The Antenna Unit Design

Figure 1(a) shows the model of the antenna unit, which consists of a resonant cavity and a rectangular waveguide. There is a 2×2 radiating wide slit on the top of the resonant cavity, and the bottom of the resonant cavity is connected vertically with the waveguide to form a feed structure. The microwave is fed vertically into the resonant cavity through the rectangular waveguide and then radiated outward through the 2×2 radiating wide slits on the top of the resonant cavity. The whole structure is simple, without superfluous structure, which can greatly increase the power capacity of the antenna unit. As shown in Figure 1(b), the maximum electric field is 10418 V/m when the input power is 1 W. According to a study [24], the metal breakdown threshold under vacuum conditions is known to be 750 kV/cm and the pressure is 10^{-3} Pa, then the power capacity of the unit under vacuum conditions is calculated to be 51.8 MW. Figures 1(c) and 1(d) show the top and front views of the antenna unit and the antenna unit's dimensional parameters. The wall thickness t of the structure is 1 mm.

The simulation results of the reflection coefficient and gain of the antenna unit obtained by using ANSYS HFSS full-wave simulation software are shown in Figure 2(a). In the required 30~31 GHz band, the reflection coefficient is less than −18 dB, and the aperture efficiency of the antenna is calculated as follows:

$$\eta = \frac{G}{4\pi A/\lambda^2} = \frac{\lambda^2 G}{4\pi A}, \tag{1}$$

$$A = (w + 2t)^2. \tag{2}$$

So, the aperture efficiency of the antenna unit by calculated as 74%. Figure 2(b) shows the radiation pattern of the antenna unit at 30.5 GHz.

3. Power Divider and 2×8 Array Design

For high-power applications, the power capacity should be considered. Figure 3 shows the electric field distribution in a rectangular waveguide of 8.636 mm × 4.318 mm. The maximum electric field is 7150.1 V/m when the input power is 1 W. Therefore, if we choose a breakdown threshold of 750 kV/cm for the metal, the power capacity is about 100 MW in a vacuum. Thus, the design goal is to reduce the field electric field strength as much as possible to make the antenna array reach the power limit of the waveguide.

3.1. Power Divider Design. To expand the designed antenna unit to a larger array, we need to redesign the feed network and at the same time, we must keep the power capacity of the antenna at a high level. Therefore, we choose the usual waveguide power divider to form the feed network, which has a higher power capacity. The divider divides into E-plane and H-plane, as shown in Figure 4, and the power capacity is about 56 MW.

Figures 5(a) and 5(b) show the reflection and transmission coefficients of the E-plane and H-plane power dividers, respectively. The reflection coefficients of both structures are less than −10 dB at 30–31 GHz, while the transmission coefficients are about −3 dB. The simulated S-parameter results prove that the structures have good transmission performance.

3.2. 2×8 Array Design. Using the mentioned antenna unit and power dividers, we get a 2×8 antenna array with a size of 30 mm × 117 mm as shown in Figure 6(a). Two 8-way waveguide power dividers feed 16 cavities, each with four radiating slits. Figure 6(b) shows the electric field distribution at 30.5 GHz, the maximum electric field is 10365 V/m, so the power capacity in a vacuum is about 50 MW.

Figure 7(a) shows the simulated results of this array. The reflection coefficient is less than −10 dB at 30–30.75 GHz,

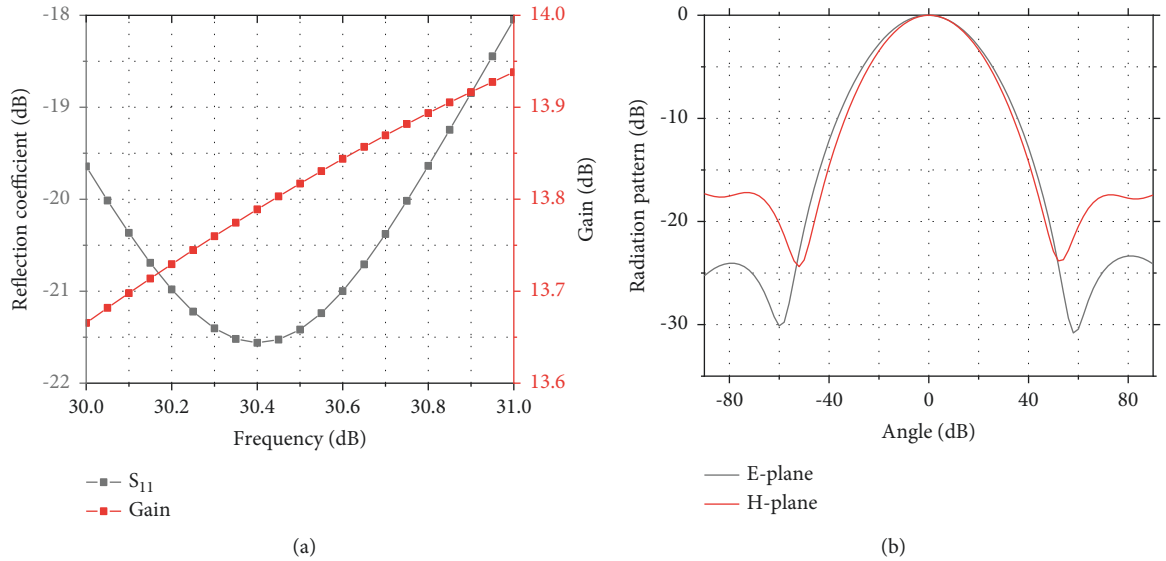

Figure 2: Simulated (a) $|S_{11}|$, gain, and (b) radiation patterns of the subarray.

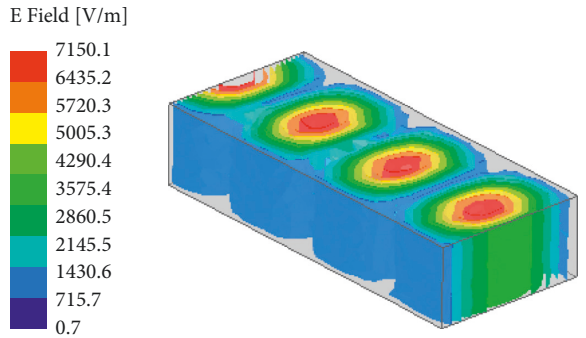

Figure 3: Electric field distribution in the rectangular waveguide.

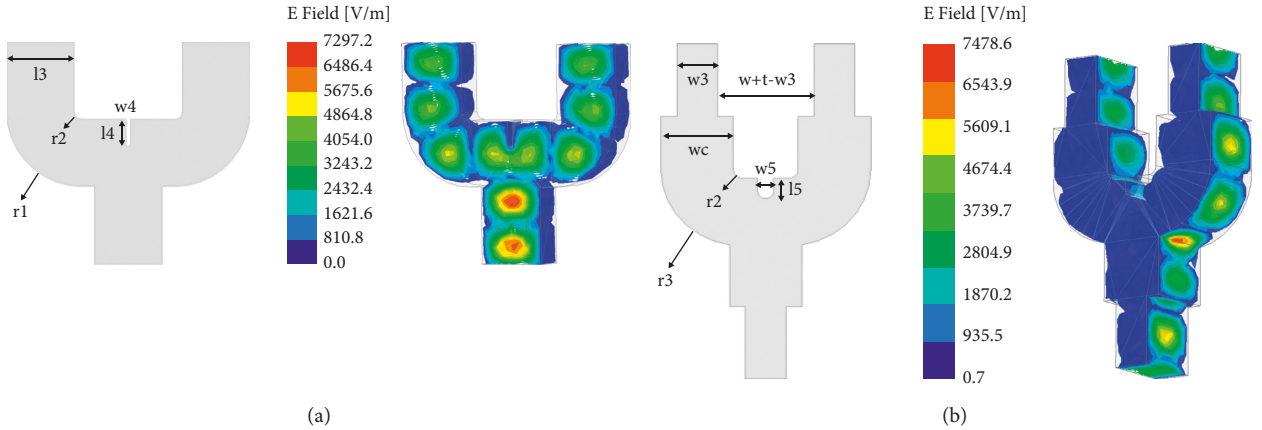

Figure 4: Schematic and electric field distribution of the (a) E-plane power divider and (b) H-plane power divider. $w3 = 4.318$ mm, $l3 = 8.636$ mm, $w4 = 0.64$ mm, $l4 = 3.26$ mm, $w5 = 1.66$ mm, $l5 = 2.03$ mm, $wc = 7.45$ mm, $t = 1$ mm, $r1 = 0.54$ mm, $r2 = 9.84$ mm, and $r3 = 8.45$ mm.

which proves the good performance of the array, and the gain of the antenna is 25.9 dB at 30.5 GHz, so its aperture efficiency is 85.3%. Figure 7(b) shows the radiation pattern of the array. The 2×8 array can be used as a subarray unit with 26 dB gain and 50 MW power capacity. Multiple subarrays can be combined into a larger array to meet the power capacity and gain requirements of antenna arrays in different scenarios.

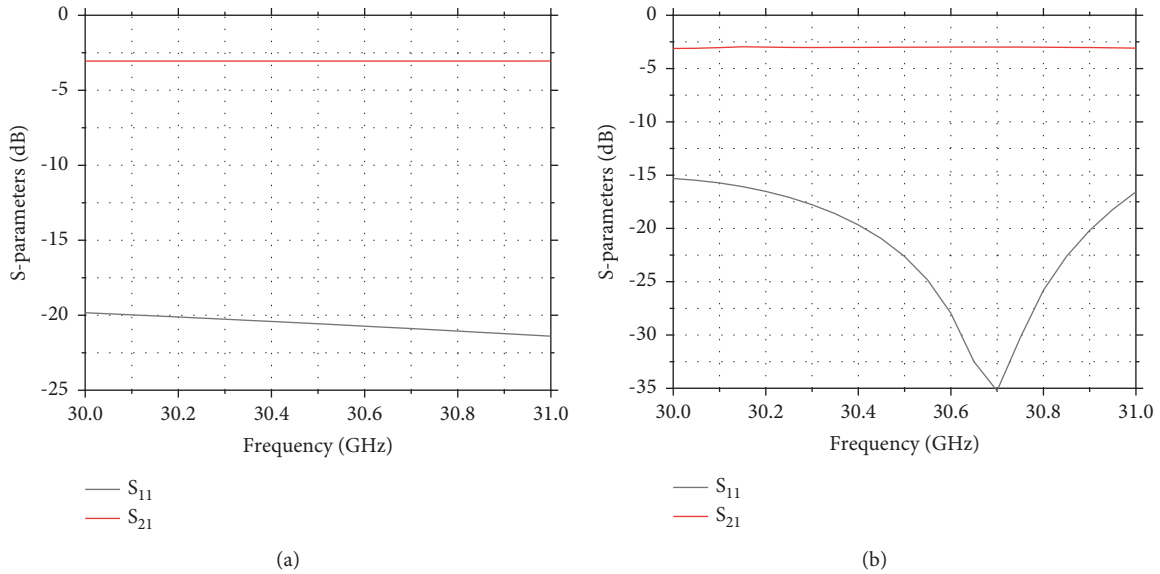

Figure 5: Simulated reflection and transmission coefficients of the (a) E-plane power divider and (b) H-plane power divider.

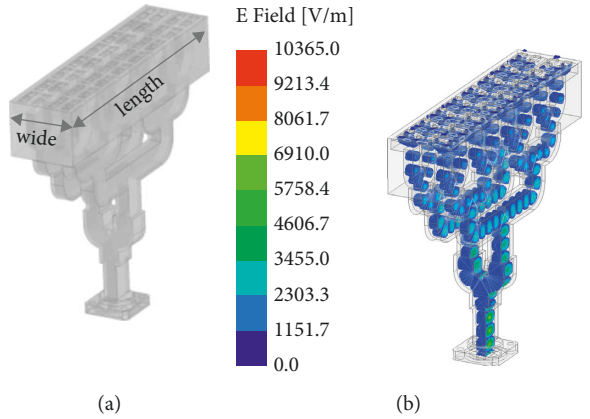

Figure 6: (a) Schematic and (b) electric field distribution of the 2 × 8 antenna array; wide = 30 mm and length = 117 mm.

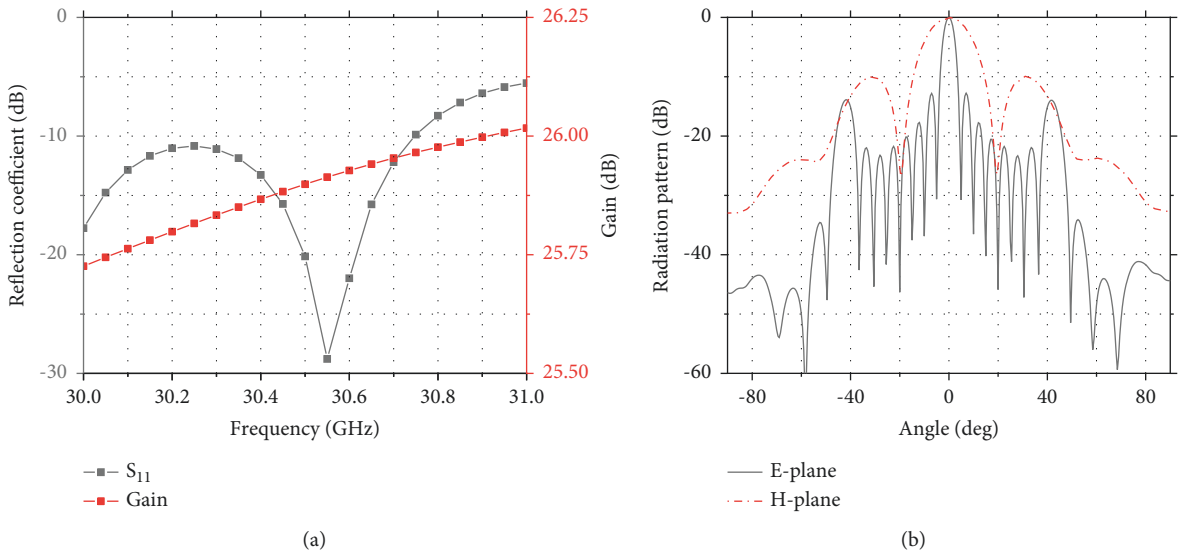

Figure 7: Simulated (a) |S11|, gain, and (b) radiation patterns of the 2 × 8 array.

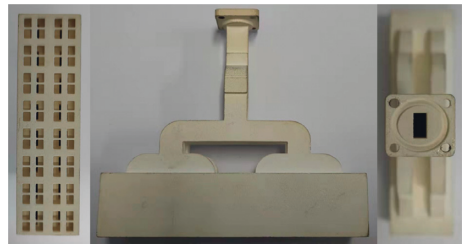

Figure 8: Photograph of the fabricated 2 × 8 array.

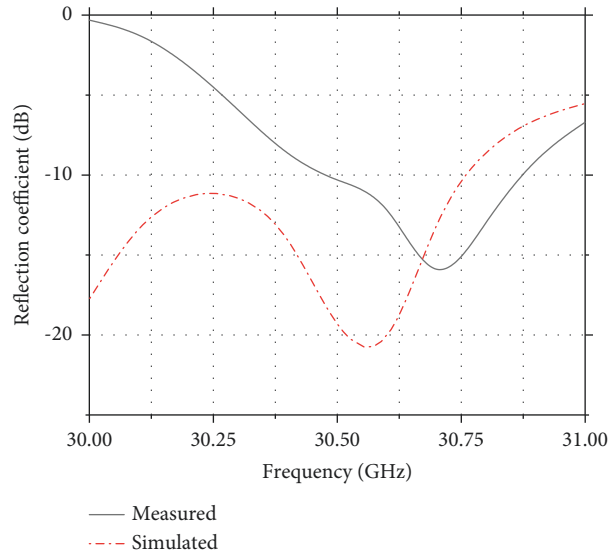

Figure 9: A comparison between the measured and simulated reflection coefficients of the 2 × 8 antenna array.

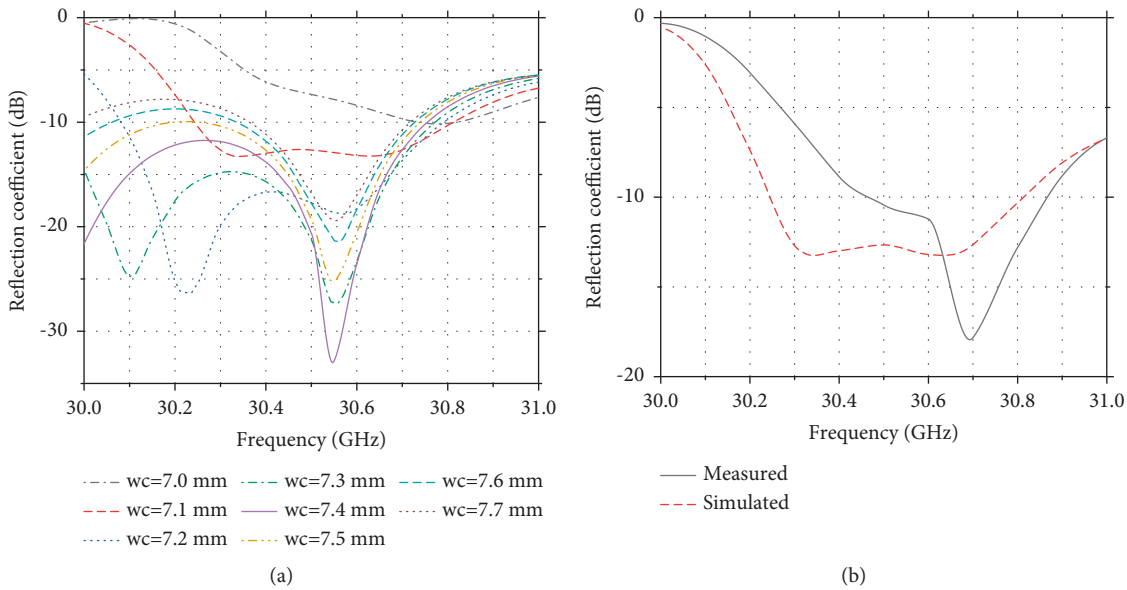

Figure 10: (a) Simulated reflection coefficients of the 2 × 8 antenna array at different *wc* values, and (b) a comparison between the measured and simulated reflection coefficients of the 2 × 8 antenna array at 7.1 mm.

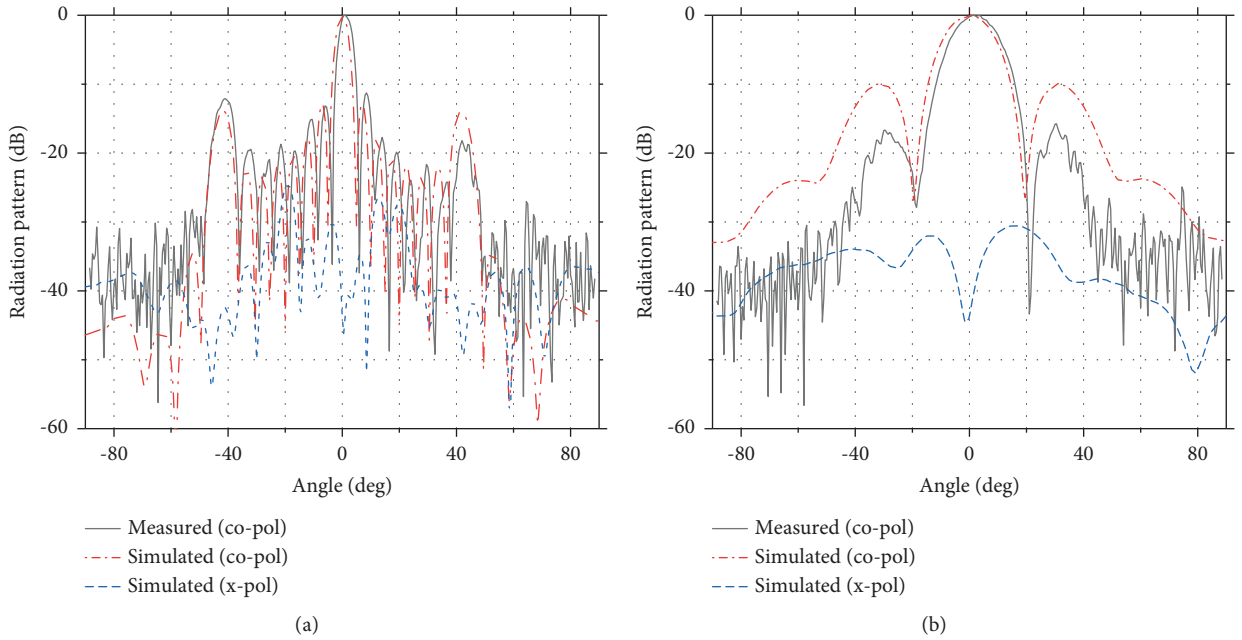

Figure 11: A comparison between the measured and simulated radiation patterns of the 2 × 8 antenna array at 30.5 GHz. (a) E-plane. (b) H-plane.

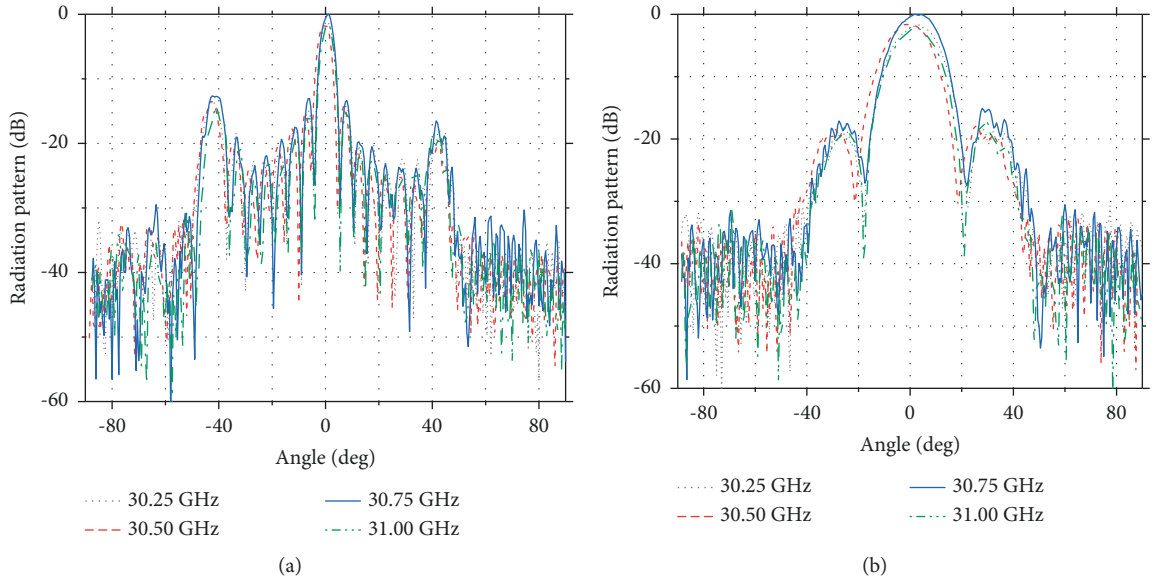

Figure 12: Radiation patterns of the 2 × 8 antenna array at 30.25, 30.5, 30.75, and 31 GHz. (a) E-plane. (b) H-plane.

4. Measurement Results

Figure 8 shows the fabricated antenna array, which is made of aluminum by 3D printed technology with a wall thickness of 1 mm. The reflection coefficients, S_{11} are shown in Figure 9. Compared with the simulated result, the measured results have a frequency shift. The center frequency is shifted by about 0.25 GHz, the offset is less than 1%, and the antenna's reflection coefficient is below −10 dB in the frequency band of 30.4–30.9 GHz. Compared to the simulated results, the bandwidth is much narrower and there is a huge difference at 30 GHz. The *wc* value of the H-plane power divider, shown in Figure 4(b), has a relatively large impact on the performance of the device, and it has the highest sensitivity. A sweeping analysis was performed for *wc* values from 7 mm to 7.6 mm, as shown in Figure 10. At 7.1 mm, the reflection coefficient of the antenna array is close to 0 at 30 GHz, which is very different from that at 7.4 mm, but in good agreement with the test results. Therefore, the *wc* values of the fabricated antennas may shift to around 7.1 mm, which, together with the effects of other performance parameters, leads to large differences between the simulated and tested results of the antennas.

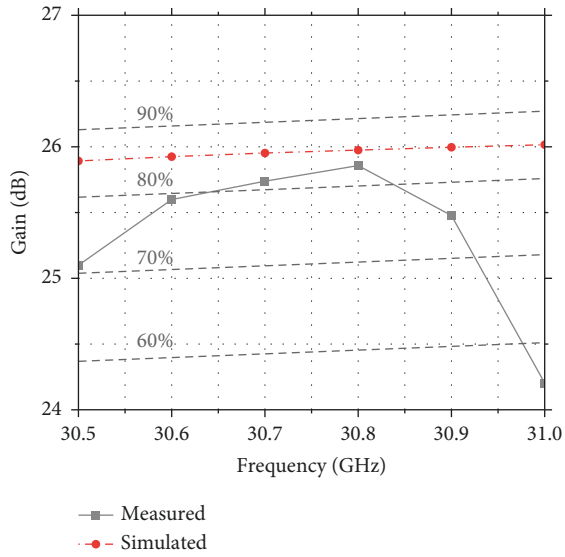

Figure 13: Measured and simulated frequency characteristics of the gain.

Table 1: Comparison with previously reported Ka-band antenna arrays.

	This work	[17]	[18]	[19]
Frequency (GHz)	**30.8**	31.5	37.5	37.5
Elements number	**2 × 8**	8 × 8	4 × 4	8 × 8
Size (mm)	$3\lambda \times 12\lambda$	99 × 138	$3.8\lambda \times 3.8\lambda$	$6.4\lambda \times 6.4\lambda$
Measured gain (dB)	**25.8**	18.74	17.8	24
Efficiency	**82.9%**	—	74.9%	41.7%

The simulated and measured radiation patterns of the antenna at the center frequency, 30.5 GHz, in the E-plane and H-plane are shown in Figure 11. The simulated and measured are in good agreement. The simulated cross-polarization level is −24.57 dB. Figures 12(a) and 12(b) show the measured radiation patterns at 30.25, 30.5, 30.75, and 31 GHz for E-plane and H-plane, respectively. The radiation patterns of the antenna are very consistent at each frequency point.

Figure 13 shows the measured and simulated frequency characteristics of the gain. The dashed lines indicate the gain at aperture efficiency of 90, 80, 70, and 60%. The gain of the antenna array is greater than 25 dB at 30.5–30.9 GHz, and the measured aperture efficiency is higher than 70%, with a maximum efficiency greater than 80%.

Finally, a comparison with previously reported Ka-band antenna arrays is shown in Table 1, and the proposed antenna array shows a high aperture efficiency.

5. Conclusions

In summary, a novel waveguide wide-slit antenna array based on 3D printed technology with high-power capacity and high efficiency is presented in this paper. A vertical transition structure with high transmission efficiency is used to connect the feed network and the radiating structure. This vertical transition structure not only increases the power capacity of the array, but also makes it more compact, and the tight arrangement of the radiating structure improves the aperture efficiency of the antenna as well as enables the planarization and miniaturization of the antenna. At 30.5–30.9 GHz, the measured gain of the antenna array is higher than 25 dB, the aperture efficiency is larger than 70%, and the highest efficiency is greater than 80% in the operating band. The simulated power capacity of the 2 × 8 array is about 50 MW in a vacuum, it can be used in high-power millimeter-wave systems.

Data Availability

No data were used to support this study.

Conflicts of Interest

The authors declare that they have no conflicts of interest.

Acknowledgments

This work was in part supported by the Science and Technology on High Power Microwave Laboratory Fund under grant no. 6142605190201.

References

[1] R. J. Barker and E. Schamiloglu, *High-power Microwave Sources and technologies*, pp. 3–14, Wiley-IEEE Press, Hoboken, NJ, USA, June 2001.

[2] E. Schamiloglu, "High power microwave sources and applications," in *Proceedings of the 2004 IEEE MTT-S International Microwave Symposium DigestIEEE Cat. No. 04CH37535*, vol. 2, IEEE, Fort Worth, TX, USA, 2004.

[3] J. Benford, J. A. Swegle, and E. Schamiloglu, *High Power microwaves*, pp. 5–20, CRC Press, Boca Raton, FL, USA, 2007.

[4] S. Li, Z. Duan, H. Huang, and Z. H. F. Z. Y. Liu, "Extended interaction oversized coaxial relativistic klystron amplifier with gigawatt-level output at Ka band," *Physics of Plasmas*, vol. 25, no. 4, Article ID 043116, 2018.

[5] S. N. Vlasov and I. M. Orlova, "Quasioptical transformer which transforms the waves in a waveguide having a circular cross section into a highly directional wave beam," *Radiophysics and Quantum Electronics*, vol. 17, no. 1, pp. 115–119, 1974.

[6] C. C. Courtney, D. E. Voss, C. E. Baum, and W. R. Prather, "A description and the measured performance of three coaxial beam-rotating antenna prototypes," *IEEE Antennas and Propagation Magazine*, vol. 44, no. 3, pp. 30–47, 2002.

[7] C. C. Courtney, "Design and numerical simulation of coaxial beam-rotating antenna lens," *Electronics Letters*, vol. 38, no. 11, pp. 496–498, 2002.

[8] Y. Rahmat-Samii, D.-W. Duan, and D. V. L. F. Giri, "Canonical examples of reflector antennas for high-power microwave applications," *IEEE Transactions on Electromagnetic Compatibility*, vol. 34, no. 3, pp. 197–205, 1992.

[9] L. Tie-zhu and H. Wen-hua, S. Hao, W. Kang-yi, L. Jia-wei, and H. Hui-jun, "Design and near field characteristic of high power microwave dual-reflector antenna," in *Proceedings of the 2012 International Conference on Microwave and Millimeter Wave Technology (ICMMT)*, vol. 5, IEEE, Shenzhen, China, May 2012.

[10] C.-W. Yuan, S.-R. Peng, T. Shu, and Z.-Q. H. Li, "Designs and experiments of a novel radial line slot antenna for high-power microwave application," *IEEE Transactions on Antennas and Propagation*, vol. 61, no. 10, pp. 4940–4946, 2013.

[11] L. Yu, C. Yuan, J. He, X. L. Zhao, Y. Sun, and C. Shen, "Design of a slot-coupled radial line helical array antenna for high power microwave applications," *AIP Advances*, vol. 7, 2017.

[12] X. L. Zhao, C. W. Yuan, L. Liu, S. Peng, Q. Zhang, and H. Zhou, "All-metal transmit-array for circular polarization design using rotated cross-slot elements for high power microwave applications," *IEEE Transactions on Antennas and Propagation*, vol. 65, no. 6, pp. 3253–3256, 2017.

[13] X. L. Zhao, C. W. Yuan, L. Liu, S. Peng, Q. Zhang, and H. Zhou, "All-metal beam steering lens antenna for high power microwave applications," *IEEE Transactions on Antennas and Propagation*, vol. 65, no. 12, pp. 7340–7344, 2017.

[14] Y. Sun, J. He, C. Yuan, and Q. Zhang, "Design and experimental demonstration of a circularly polarized mode converter for high-power microwave applications," *Review of Scientific Instruments*, vol. 89, no. 8, Article ID 084701, 2018.

[15] Y. Sun, J. He, C. Yuan, and Q. X. L. Zhang, "*Ku*-band radial-line continuous transverse stub antenna with transmit-array lens for high-power microwave application," *IEEE Transactions on Antennas and Propagation*, vol. 68, no. 3, pp. 2050–2059, 2020.

[16] X. Zhao, C. Yuan, and J. Zhang, Q. Zhang, "Design of a beam scanning metamaterial antenna with polarization transform for high-power microwave application," *Microwave and Optical Technology Letters*, vol. 62, October 2020.

[17] B. Liu, W. Hong, Z. Kuai, and X. G. J. H. K. Yin, "Substrate integrated waveguide (SIW) monopulse slot antenna array," *IEEE Transactions on Antennas and Propagation*, vol. 57, no. 1, pp. 275–279, 2009.

[18] T. Y. Tian Yang Yang, W. Wei Hong, and Y. Yan Zhang, "Wideband millimeter-wave substrate integrated waveguide cavity-backed rectangular patch antenna," *IEEE Antennas and Wireless Propagation Letters*, vol. 13, pp. 205–208, 2014.

[19] X. Jiang, F. Jia, and Y. P. J. X. Huang, "Ka-band 8 × 8 low-sidelobe slot antenna array using a 1-to-64 high-efficiency network designed by new printed RGW technology," *IEEE Antennas and Wireless Propagation Letters*, vol. 18, no. 6, pp. 1248–1252, 2019.

[20] J. Wei, Z. N. Chen, X. J. Shi, and J. au, "Compact substrate integrated waveguide slot antenna array with low back lobe," *IEEE Antennas and Wireless Propagation Letters*, vol. 12, pp. 999–1002, 2013.

[21] N. Shahrubudin, T. C. Lee, and R. Ramlan, "An overview on 3D printing technology: technological, materials, and applications," *Procedia Manufacturing*, vol. 35, pp. 1286–1296, 2019.

[22] D. J. Horst, C. A. Duvoisin, and R. de Almeida Vieira, "Additive manufacturing at Industry 4.0: a review," *International journal of engineering and technical research*, vol. 8, no. 8, pp. 27–30, 2018.

[23] B. Zhang and H. Zirath, "Metallic 3-D printed rectangular waveguides for millimeter-wave applications," *IEEE Transactions on Components, Packaging, and Manufacturing Technology*, vol. 6, no. 5, pp. 796–804, 2016.

[24] R. A. Jameson, "High-brightness H-accelerators," in *Proceedings of the particle accelerator conference*, vol. 903, pp. 16–19, Washington, DC, USA, March 1987.